Hindawi
International Journal of Antennas and Propagation
Volume 2022, Article ID 9260843, 8 pages
https://doi.org/10.1155/2022/9260843

Research Article

Realization of Low Cross-Polarization Level for GF-3 SAR Antenna

Jian Mi, Hongbing Sun, Guodong Song, Ying Xing, and Xuhao Zhao

Nanjing Research Institute of Electronics Technology, Nanjing 210039, China

Correspondence should be addressed to Jian Mi; mijian@pku.edu.cn

Received 1 April 2022; Accepted 26 May 2022; Published 7 June 2022

Academic Editor: Miguel Ferrando Bataller

Copyright © 2022 Jian Mi et al. This is an open access article distributed under the Creative Commons Attribution License, which permits unrestricted use, distribution, and reproduction in any medium, provided the original work is properly cited.

In the polarimetric synthetic aperture radar (PolSAR) system, crosstalk error is the key parameter for polarimetric imaging. The source of crosstalk is mostly from the cross-polarization level of the SAR antenna subsystem. To meet the requirements of PolSAR observing modes, a low cross-polarization level under −35 dB is realized for the SAR antenna of the GF-3 satellite. In this paper, we will describe the principles and methods for implementation of low cross-polarization level. The two polarized RF chains are totally independent to ensure high isolation, and a dual-polarized waveguide slot antenna subarray is designed with a low cross-polarization level. Besides, the low taper efficiency of the cross-polarization pattern contributes to reduce the cross-polarization, showing the advantage of the phased array antenna in the PolSAR system. The paper also displays the measured results of cross-polarization for the GF-3 SAR antenna. The study gains a better understanding of the cross-polarization pattern for phased array antenna. The methods utilized here can be extended to other polarimetric SAR systems.

1. Introduction

GF-3 satellite was successfully launched on August 10, 2016. It is the first fully polarimetric synthetic aperture radar imaging satellite in China [1], and 12 observing modes are designed to meet the multiuser technical requirements [1, 2]. Especially, the SAR system has three polarimetric SAR imaging modes: quad-pol stripmap (Q), wide quad-pol stripmap (WQ), and wave (WV), making it efficient in geographical interpretation and quantitative research. In order to reduce satellite revisit time and improve system reliability, GF-3B and GF-3C were launched in 2021 and 2022, respectively, and thus, a radar constellation has been established.

Polarization is an inherent property of electromagnetic waves, describing the time-varying direction and relative magnitude of the electric field vector. It is classified as linear polarization, circular polarization, and elliptical polarization. The PolSAR system of GF-3 works by measuring the scattering information of the Earth's surface with two linear polarization microwaves [3]. For example, it transmits vertical polarization wave and receives echoes in vertical and horizontal polarizations simultaneously. Through the signal processing of polarimetric echoes, we can get more information about targets and obtain a more sophisticated physical interpretation of the scattering mechanism, which is convenient for target classification and recognition. PolSAR plays an irreplaceable role in the comprehensive perception of target characteristics.

In the PolSAR system, the crosstalk error describes the purity of the polarization signal and increases the magnitude of the cross-pol images relatively [3–5]. For geophysical parameter inversion research and multitemporal studies over large areas such as GF-3 satellite, the crosstalk should be less than -35 dB. The source of crosstalk is mostly from the cross-polarization level of the SAR antenna subsystem. Table 1 shows the comparison of SAR antennas between PolSAR satellites [6–11]. For the C-band PolSAR system, the polarization isolation of GF-3 is better than Envista, RADARSAT-2, Sentinel-1, and RCM, providing strong support for high-quality polarimetric imaging.

In the design of radiation antenna elements, the microstrip antenna is adopted by Envista, RADARSAT-2, and RCM. But it is difficult to realize a low cross-polarization level by microstrip antenna, and the polarization isolation of these satellites is below 30 dB. The radiation antenna of Sentinel-1 is a waveguide antenna, which is better for

Table 1: Characteristics comparison of SAR antennas between PolSAR satellites.

Satellite	Frequency (GHz)	Polarization isolation	Antenna size	Launch year
Envista	5.331	>25 dB	10 m × 1.3 m	2002
ALOS2	1.27	>35 dB	8.9 m × 3.1 m	2006
RADARSAT-2	5.405	>25 dB	15 m × 1.37 m	2007
TerraSAR-X	9.65	>25 dB	4.8 m × 0.8 m	2007
Sentinel-1	5.405	>30 dB	12.3 m × 0.82 m	2014
GF-3	5.40	>35 dB	15 m × 1.23 m	2016
RCM	5.405	>28 dB	6.75 m × 1.38 m	2019

polarization isolation, but the transmit RF distribution network is shared by two polarizations.

In order to reduce the cross-polarization level for the GF-3 SAR antenna, a dual-polarized waveguide slot antenna subarray is designed, and the H-Pol and V-Pol RF chains are totally independent. Previous papers about antenna cross-polarization all focus on the design of radiation antenna, but not from a system perspective. This paper will describe the implementation method of low cross-polarization from three aspects: system design, radiation antenna subarrays, and a quantitative study on the taper efficiency of cross-polarization pattern, which contributes to reduce the cross-polarization level. The cross-polarization test results indicate that these methods are effective, and a large phased array antenna has the advantage of a low cross-polarization level compared to a reflector antenna, which is also widely used in spaceborne SAR systems.

In this paper, the system design scheme for the SAR antenna is described in Section 2. Section 3 describes the design of the radiation antenna subarray, followed by the discussion on the taper efficiency of the cross-polarization pattern in Section 4. The measured results are presented and analyzed in Section 5, and the conclusions are presented in Section 6.

2. System Design

The SAR antenna of GF-3 is composed of 1536 transmit/receive (T/R) channels: 24 in azimuth and 32 in elevation for each polarization.

In the design of RF chains, there exist two solutions: isolated H/V T/R chains and shared H/V T/R chains. The schematic diagrams of the two schemes are shown in Figure 1. The internal calibration network, which is used to monitor the amplitude and phase change of each T/R channel, is shared by H_Pol and V_Pol chains. For the isolated solution, the H-Pol and V-Pol RF chains are independent, which is convenient to realize high polarization isolation but not easy for the realization of antenna lightweight. For the shared solution, the transmit chains of H and V polarizations are shared, and the receive chains are independent. This solution is easy to reduce the amount of high-power amplifiers and the antenna weight, but the isolation between two polarizations is limited by the performance of the high-power switch chip, which is hard to realize high isolation and also with high insertion loss and low reliability.

In order to achieve high polarization isolation of the antenna system, we adopt the isolated H/V chains scheme. The isolation between H_Pol and V_Pol RF chains is

$$a\_\text{cross} = -(2 \cdot (C + L) - 3)\ (\text{DB}), \tag{1}$$

where C is the coupling coefficient of the directional coupler for the internal calibration network, and L is the insertion loss from the coupler to the 1 : 2 power divider. In our system, $C = -25$ dB, and $L = -0.5$ dB. The isolation is better than 54 dB and is much higher than the requirement of 35 dB. The isolated scheme also improves the reliability of the PolSAR system: the failure of one power amplifier or switch only affects the performance of one polarization.

3. Antenna Subarray

For the advantage of high radiation efficiency, low cross-polarization level, high thermal stability, and cost-effectiveness, a dual-polarized waveguide slot antenna subarray is adopted, instead of the microstrip antenna. The picture of the waveguide antenna and schematic diagram of the array are shown in Figures 2(a) and 2(b). The antenna array is composed of $24 \times 32 = 768$ antenna subarrays. The size of each subarray is 625 mm in azimuth 38 mm in elevation.

The structure of the waveguide slot antenna is shown in Figures 2(c) and 2(d). The material of the antenna is aluminium. Each subarray is composed of a vertically polarized waveguide slot antenna and a horizontally polarized waveguide slot antenna [12–17]. Each polarization antenna with 16 radiating slots is divided into two parts and fed by a waveguide divider (waveguides 1 and 3) to broaden the bandwidth. The disturbance blocks are used to change the electric field distribution near the slots, making the slots radiate at the center of the waveguide wall. The position of the blocks at adjacent slots is contrary because the path difference of adjacent slots is a half wavelength.

Besides, the design of ridge waveguide is aimed to reduce the size and weight, and the two independent polarized antennas are physically isolated. Differing from the common inclined slots in waveguide antenna, the straight slots effectively reduce the mutual coupling between the two polarized antennas and enhance the polarization isolation of the antenna subarray.

Figures 2(e) to 2(g) show the measured VSWR and cross-polarization level of the dual-polarized waveguide antenna in azimuth at 5.4 GHz. The VSWR of two polarizations is under 1.6 within the working bandwidth (5.25 GHz to 5.55 GHz). In the main lobe, the cross-

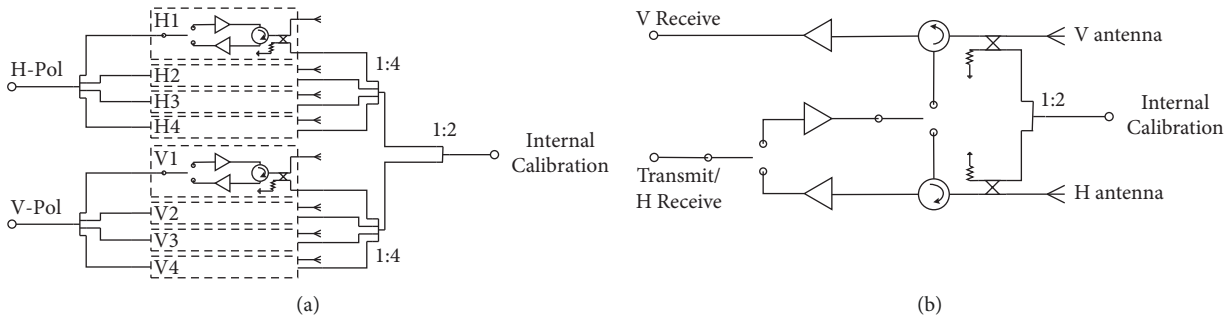

Figure 1: Schematic diagram of RF chains schemes. (a) Isolated H/V T/R chains. (b) Shared H/V T/R chains.

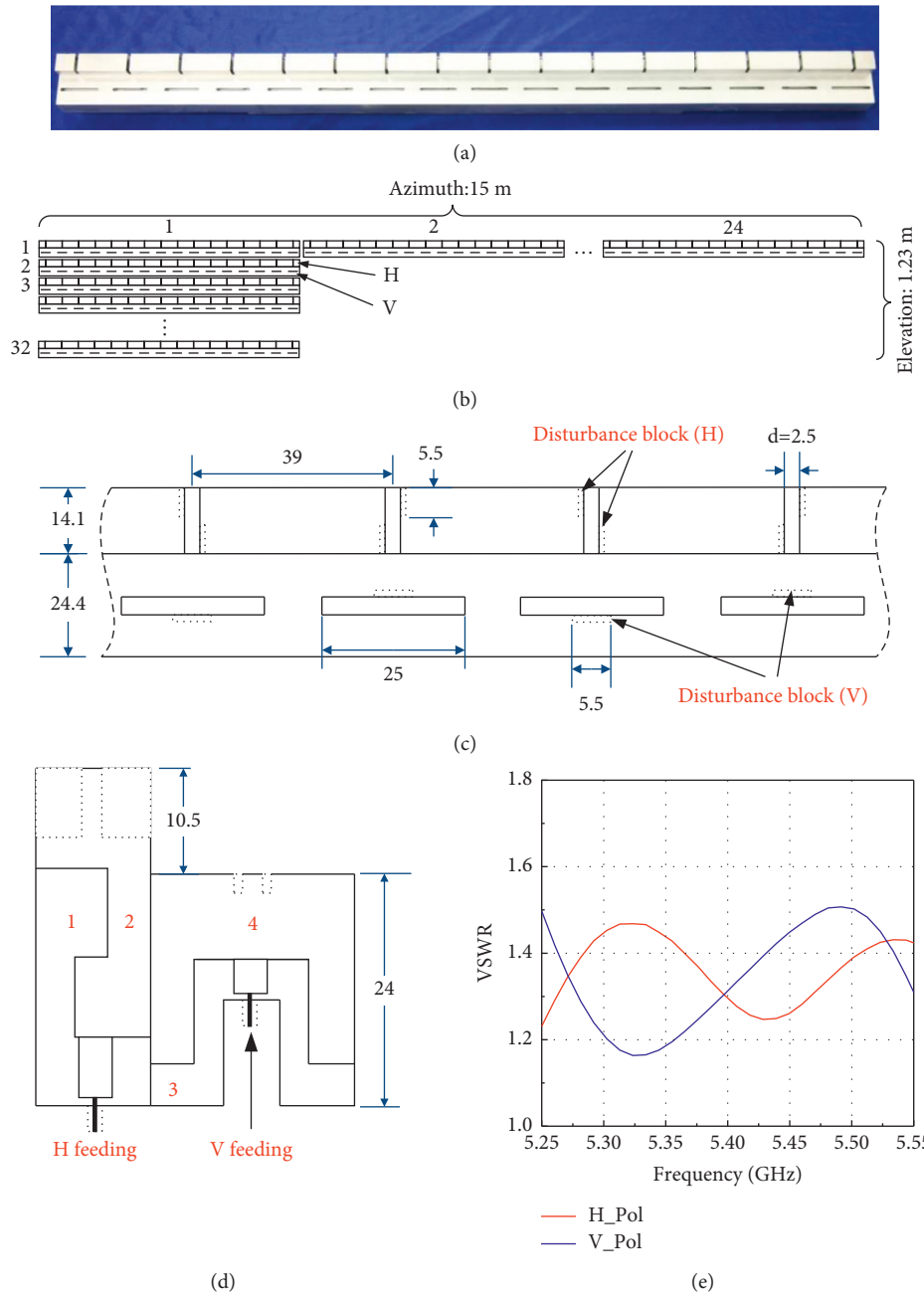

Figure 2: Continued.

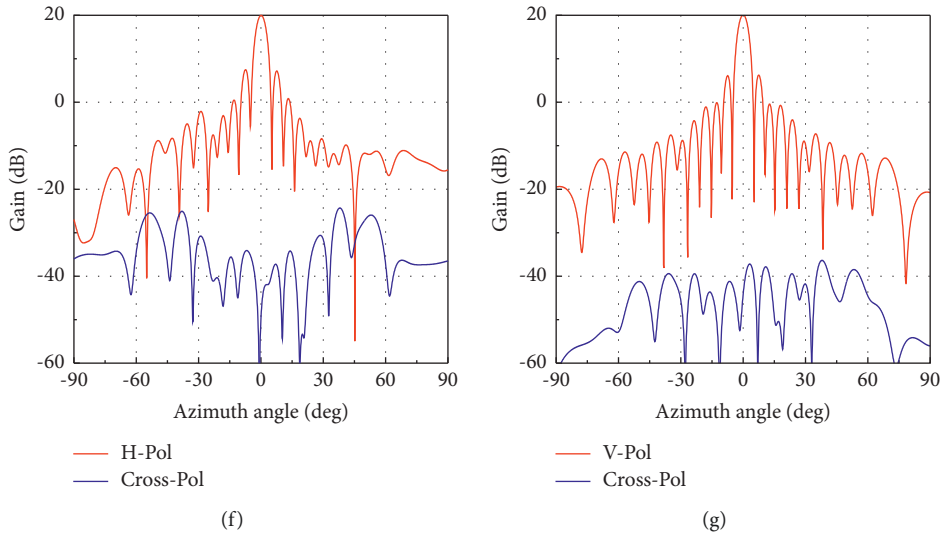

Figure 2: (a) Picture of the waveguide slot antenna subarray. (b) Schematic diagram of the large antenna array. (c) Top view of the antenna subarray. (d) Section view of the antenna subarray. The unit in (c) and (d) is millimeter. (e) The measured VSWR of the dual-polarized antenna. (f) Cross-polarization level of H polarized waveguide antenna. (g) Cross-polarization level of V polarized waveguide antenna.

polarization level is lower than −40 dB compared to the copolarization level. Besides, the radiation efficiency is greater than 80%. The design of the waveguide antenna subarray is very effective in reducing the cross-polarization level of the SAR antenna.

4. Low Taper Efficiency of Cross-Polarization

For active phased array antennas, the copolarization radiated pattern F is calculated by [18]

$$\mathrm{F\_co}(u,v) = \sum_{m=1}^{M}\sum_{n=1}^{N} f_{mn}(u,v)\cdot a_{mn}\cdot \exp\left[jk\left(x_m u + y_n v\right)\right], \tag{2}$$

where M and N are the amount of antenna subarrays in each dimension, $f_{mn}(u, v)$ is the pattern of antenna subarray, a_{mn} is the complex excitation coefficient of each T/R channel, x_m and y_n are the position of antenna subarrays, k is the wave vector.

In the GF-3 SAR antenna system, the cross-polarization radiated pattern F_cross is

$$\begin{aligned}\mathrm{F\_cross}(u,v) = \sum_{m=1}^{M}\sum_{n=1}^{N}\left[f\_\mathrm{cross}_{mn}(u,v) + f_{mn}(u,v)\cdot a\_\mathrm{cross}_{mn}\right] \\ \cdot a_{mn}\cdot \exp\left[jk\left(x_m u + y_n v\right)\right].\end{aligned} \tag{3}$$

In this equation, $f\_\mathrm{cross}_{mn}(u, v)$ is the cross-polarization pattern of the antenna subarray, a_cross_{mn} is the crosstalk in the T/R channel, and the value is under −54 dB (equation (1)). Thus, the cross-polarization level is mostly decided by $f\_\mathrm{cross}_{mn}(u, v)$.

For copolarization, the patterns of each antenna subarray $f_{mn}(u, v)$ are almost the same, and the array efficiency is characterized by taper efficiency [18].

$$\varepsilon_{\mathrm{T}} = \frac{\left|\sum a_{mn}\right|^2}{M\cdot N\sum\left|a_{mn}\right|^2}. \tag{4}$$

But, for cross-polarization, the cross-polarization patterns of each antenna subarray $f\_\mathrm{cross}_{mn}(u, v)$ are diverse, which is equivalent to the diversity of excitation coefficient a_{mn}. Thus, the taper efficiency of the cross-polarization pattern is lower than the copolarization pattern, reducing the cross-polarization level of the array. For a large antenna array, the low cross-polarization level is not only the contribution from radiation antenna elements but also from channel isolation (a_cross_{mn}) and taper efficiency (ε_T).

To analyze the cross-polarization pattern of the antenna subarray quantitatively, we simulate the electric field of copolarization and cross-polarization with the change of

Table 2: Simulated electric field of copolarization and cross-polarization vs. waveguide slot width error.

Slot width error (mm)	Copol amp (dB)	Copol phase (deg)	Cross-Pol amp (dB)	Cross-Pol phase (deg)
−0.08	32.40	−81.0	−27.65	−29.68
−0.06	32.11	−78.3	−21.43	−165.82
−0.04	32.26	−84.38	−13.36	−144.49
−0.02	32.13	−77.87	−20.68	−87.60
0	32.12	−81.72	−11.09	12.83
0.02	32.36	−79.22	−15.76	−130.44
0.04	32.17	−77.39	−20.15	−124.88
0.06	32.44	−74.9	−18.2	4.55
0.08	32.38	−75.11	−18.68	−129.29

H-Pol waveguide slot width (parameter d in Figure 2(c)) by HFSS software. The electric field value at the boresight direction is shown in Table 2. The slot width error is from −0.08 mm to +0.08 mm. For the copolarization pattern, the maximum amplitude change is +0.32 dB, and the phase changes from −2.7 degree to +6.8 degree. For the cross-polarization pattern, the maximum amplitude change is −16.6 dB, and the phase changes from −178.6 degree to −8.3 degree. From the simulated results, we can conclude that the copolarization electric field of antenna subarray is robust and keeps nearly constant with manufacturing error, but the cross-polarization electric field is very sensitive and varies dramatically with the error. A large phased array antenna has the advantage of low cross-polarization compared to the reflector antenna for the existence of antenna subarray manufacturing error.

5. Results

The cross-polarization level of the GF-3 SAR antenna is measured in a planar near-field system. We take H-polarization for example. The antenna is set to the receiving state of H-polarization. First, we measure the near field of the copolarization. Then, we rotate the waveguide probe for 90 degree and get the near field of the cross-polarization. The copolarization and cross-polarization patterns are calculated by the FFT method. Cross-polarization of the probe should be lower than −35 dB, and the angle error of the probe is less than 0.1° to keep a high polarization purity of the receiving signal.

The copolarization and cross-polarization results of the boresight beam are shown in Figure 3. For simplicity, only the elevation patterns at the central frequency (5.4 GHz) are displayed. The cross-polarization level of H-polarization and V-polarization is under −47 dB and −50 dB, respectively. The peak positions of the copolarization and cross-polarization patterns are well aligned, which is the contribution of the array factor.

In order to study the mechanism of cross-polarization pattern quantitatively, we transform the measured near-field results to aperture-field based on plane wave spectrum theory [19]. Figure 4 shows the amplitude and phase distribution of the aperture field for H-polarization and cross-polarization at 5.4 GHz. For copolarization, the amplitude fluctuation of the SAR antenna is less than 6 dB, and the phase fluctuation is about 30 degree, showing good amplitude and phase consistency of the aperture field and high taper efficiency of the copolarization pattern. In Figure 4(b), the boundary of antenna subarrays in the azimuth direction is very evident, indicating the discontinuity of the electric field between two subarrays, where a 6 mm width splicing seam exists.

For cross-polarization in Figures 4(c) and 4(d), the amplitude and phase distribution on the antenna surface are messy compared to the aperture field of copolarization. The amplitude fluctuation is greater than 40 dB, and the phase fluctuation is from −180 degree to 180 degree, showing low taper efficiency of the cross-polarization pattern. In Figure 4(c), we can see two areas with strong electric field intensity at the antenna boundary in the elevation direction, indicating a strong edge effect caused by the antenna frame which is made of carbon fiber-reinforced plastics. Besides, the splicing seam of antenna subarrays in the azimuth direction can raise the cross-polarization field amplitude slightly.

To study the array taper efficiency of copolarization and cross-polarization pattern more clearly, we transform the aperture field to the complex field value of all waveguide subarrays. It is realized by summing up the aperture electric field corresponding to the specified waveguide subarray. The amplitude and phase of copolarization and cross-polarization for all subarrays are shown in Figure 5. For copolarization, the amplitude of all subarrays is within 2.5 dB, and the phase is within 14 degree, and the calculated taper efficiency is 0.997. But, for cross-polarization, the amplitude range is greater than 30 dB, the phase changes from −180 degree to 180 degree, and the taper efficiency is 0.21. The results confirm that the cross-polarization pattern of every antenna subarray is very sensitive and varies dramatically with manufacturing errors. In Figure 5(a), the average amplitude of copol is about 40 dB higher than the average amplitude of cross-pol, and the contribution from taper efficiency is 7 dB (0.997/0.21), leading to the cross-polarization level close to -47 dB shown in Figure 3(a).

The realization of low cross-polarization for phased array antenna is not only the contributions of antenna subarrays but also the effects of low array taper efficiency for the cross-polarization pattern.

To estimate the performance of polarimetric SAR imaging modes, we measure the cross-polarization level of some beams designed for polarimetric imaging mode. The results are shown in Table 3. The signal bandwidth of PolSAR

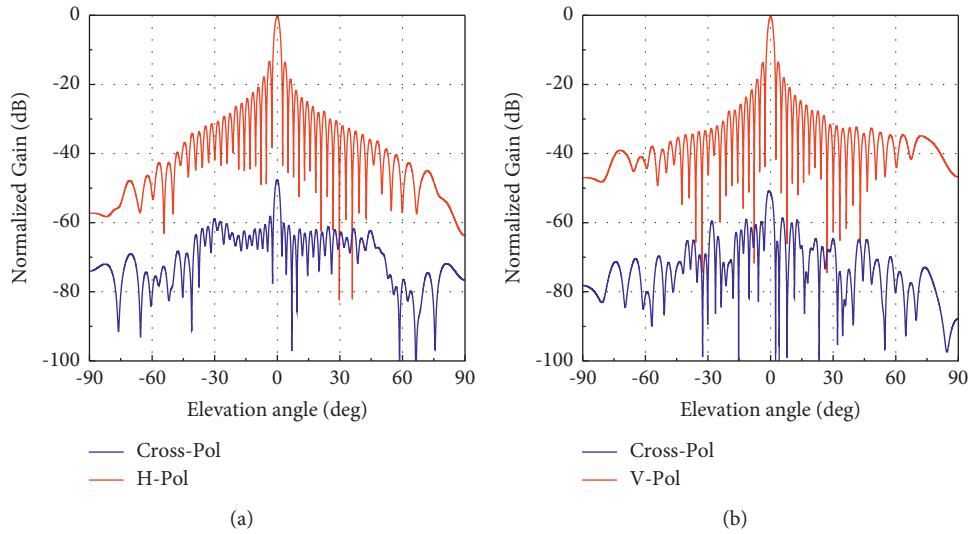

Figure 3: (a) Measured H-polarization pattern and cross-polarization. (b) Measured V-polarization pattern and cross-polarization.

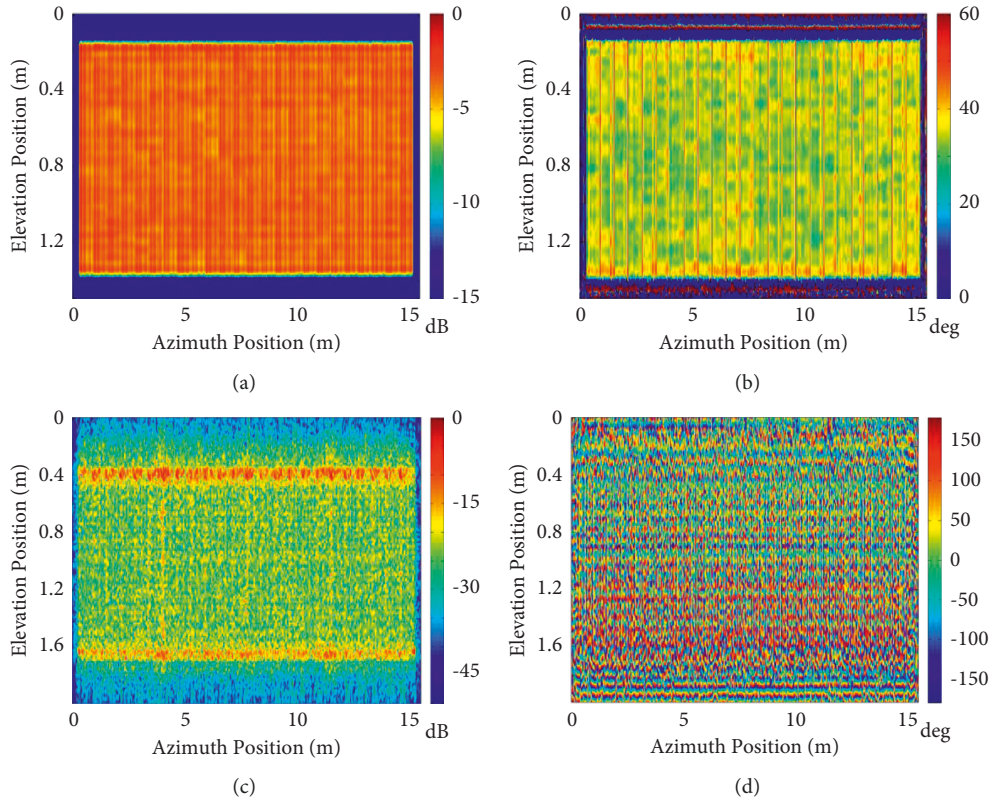

Figure 4: (a) Normalized amplitude of the aperture field for H-polarization. (b) Phase of the aperture field for H-polarization. (c) Normalized amplitude of the aperture field for cross-polarization. (d) Phase of the aperture field for cross-polarization.

mode is 60 MHz, so the results covering 120 MHz bandwidth are enough to evaluate the cross-polarization performance. For H-polarization, the maximum cross-polarization level is −37.3 dB. The cross-polarization level rises as the antenna elevation look angle increases. For V-polarization, the cross-polarization levels are lower than −40.3 dB, not showing a close relationship with the elevation look angle. The cross-polarization of the waveguide probe and the angle error of the measurement system will raise the measured cross-polarization value, so we can conclude that the actual cross-polarization of the antenna is lower than the measured results. In summary, the measured isolation between two

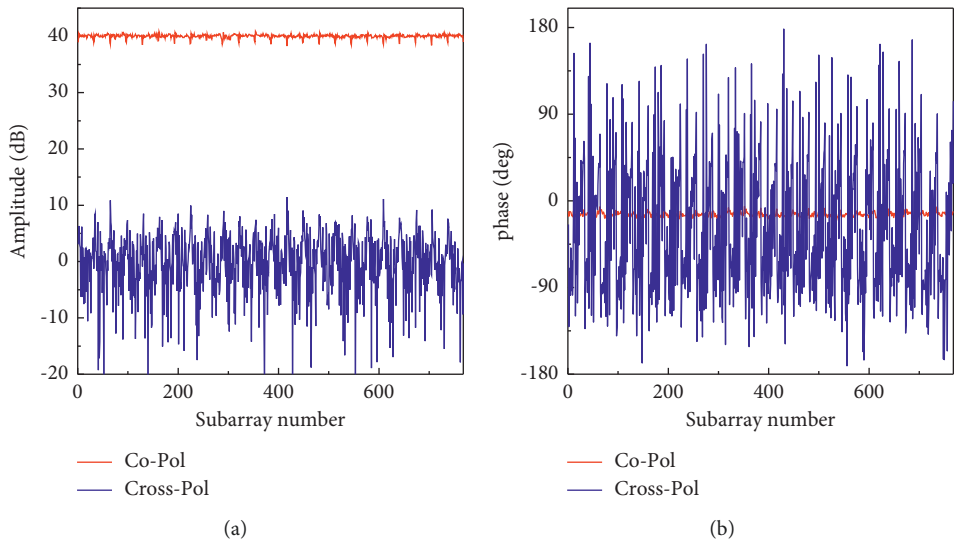

Figure 5: Calculated field value of all waveguide subarrays. (a) Amplitude for copolarization and cross-polarization. (b) Phase for copolarization and cross-polarization.

Table 3: Cross-polarization level results of Q mode and WQ mode.

Beam number	Elvation angle/deg	Cross-polarization level (H-pol) (dB)			Cross-polarization level (V-pol) (dB)		
		5.34 GHz	5.40 GHz	5.46 GHz	5.34 GHz	5.40 GHz	5.46 GHz
Q1	−12.6	−38.4	−38.9	−41.2	−41.4	−43.8	−40.3
Q14	3.25	−44.2	−45.4	−46.0	−43.8	−45.1	−46.9
Q20	6.8	−42.4	−42.3	−42.7	−49.0	−45.6	−44.0
Q23	8.57	−42.0	−41.6	−41.3	−45.3	−42.5	−43.7
Q28	11.25	−39.8	−39.4	−39.4	−45.5	−44.9	−41.1
WQ1	−12.7	−37.6	−37.3	−39.1	−41.1	−44.5	−38.0
WQ3	−7.4	−43.2	−43.4	−45.9	−41.2	−41.4	−43.4
WQ5	−3.77	−49.4	−44.4	−49.3	−46.9	−44.7	−43.9
WQ10	2.74	−44.6	−45.4	−46.7	−43.3	−44.5	−47.0
WQ13	7.3	−42.4	−42.2	−42.0	−48.1	−44.1	−43.4

polarizations is much higher than the PolSAR requirement of 35 dB; thus, the crosstalk error of the PolSAR system can be neglected.

6. Conclusion

GF-3 is the first C-band PolSAR satellite in China. Much effort has been made to reduce the cross-polarization level to ensure high accuracy for polarimetric imaging. This paper describes the principle and implementation method of low cross-polarization for GF-3 SAR antenna from antenna system design, radiation antenna subarray, and the low array taper efficiency for the cross-polarization pattern. The pattern of copolarization and cross-polarization for beams used in polarimetric modes is measured in a planar near-field system.

The measured results and analysis show that the cross-polarization level of PolSAR modes is lower than −35 dB, and a large phased array antenna has the advantage of low cross-polarization compared to a reflector antenna, because of the low array taper efficiency of the cross-polarization pattern. The employment of waveguide slot antenna and polarization-isolated RF chains is highly effective in reducing the antenna cross-polarization level. The study gains a better understanding of cross-polarization for large phased array antenna and can be used in other PolSAR systems.

Data Availability

The data used to support the findings of this study are available from the corresponding author upon request.

Conflicts of Interest

The authors declare that they have no conflicts of interest.

References

[1] Q. Zhang and Y. Liu, "Overview of Chinese first C band multi-polarization SAR satellite GF-3," *Aerospace China*, vol. 18, no. 3, pp. 22–31, 2017.

[2] J. Sun, W. Yu, and Y. Deng, "The SAR payload design and performance for the GF-3 mission," *Sensors*, vol. 17, no. 10, Article ID 2419, 2017.

[3] Y. Chang, P. Li, J. Yang, J. Zhao, L. Zhao, and L. Shi, "Polarimetric calibration and quality assessment of the GF-3 satellite images," *Sensors*, vol. 18, no. 2, p. 403, 2018.

[4] G. Sun, Z. Li, L. Huang, Q. Chen, and P. Zhang, "Quality analysis and improvement of polarimetric synthetic aperture radar (SAR) images from the GaoFen-3 satellite using the Amazon rainforest as an example," *International Journal of Remote Sensing*, vol. 42, no. 6, pp. 2131–2154, 2021.

[5] S. Kumar, A. Babu, S. Agrawal, U. Asopa, S. Shukla, and A. Maiti, "Polarimetric calibration of spaceborne and airborne multifrequency SAR data for scattering-based characterization of manmade and natural features," *Advances in Space Research*, vol. 69, no. 4, pp. 1684–1714, 2022.

[6] R. Touzi, P. W. Vachon, and J. Wolfe, "Requirement on antenna cross-polarization isolation for the operational use of C-band SAR constellations in maritime surveillance," *IEEE Geoscience and Remote Sensing Letters*, vol. 7, no. 4, pp. 861–865, 2010.

[7] R. Touzi and M. Shimada, "Polarimetric PALSAR calibration," *IEEE Transactions on Geoscience and Remote Sensing*, vol. 47, no. 12, pp. 3951–3959, 2009.

[8] J. Uher, C. Grenier, and G. Lefebvre, "RADARSAT-2 SAR antenna," *Canadian Journal of Remote Sensing*, vol. 30, no. 3, pp. 287–294, 2004.

[9] W. Pitz haus and D. Miller, "The TerraSAR-X satellite," *in IEEE Transactions on Geoscience and Remote Sensing*, vol. 48, no. 2, pp. 615–622, 2004.

[10] F. Rostan, S. Riegger, M. Huchler, R. Croci, and R. Torres, "Sentinel-1 C-SAR instrument design," in *Proceedings of the Int. Geosci. Remote Sens Symp*, Aachen, Germany, June 2010.

[11] A. A. Thompson, "Innovative capabilities of the RADARSAT constellation mission," in *Proceedings of the Proc. EUSAR Conf*, Aachen, Germany, June 2010.

[12] W. Wang, J. Jin, J.-G. Lu, and S.-S. Zhong, "Waveguide slotted antenna array with broadband, dual-polarization and low cross-polarization for X-band SAR applications," in *Proceedings of the IEEE International Radar Conference*, pp. 653–656, Arlington, VA, May 2005.

[13] W. Wang, J. Jin, X.-L. Liang, and Z.-H. Zhang, "Broadband dual polarized waveguide slotted antenna array," in *Proceedings of the IEEE Antennas and Propagation Society International Symposium*, pp. 2237–2240, Albuquerque, NM, July 2006.

[14] D. Kim, M. Zhang, J. Hirokawa, and M. Ando, "Design and fabrication of a dual-polarization waveguide slot array antenna with high isolation and high antenna efficiency for the 60 GHz band," *IEEE Transactions on Antennas and Propagation*, vol. 62, no. 6, pp. 3019–3027, 2014.

[15] J. Lu, H. Zhang, W. Wang et al., "Broadband dual-polarized waveguide slot filtenna array with low cross polarization and high efficiency," *IEEE Transactions on Antennas and Propagation*, vol. 67, no. 1, pp. 151–159, 2019.

[16] M. Chen, X.-C. Fang, W. Wang, H.-T. Zhang, and G.-L. Huang, "Dual-band dual-polarized waveguide slot antenna for SAR applications," *IEEE Antennas and Wireless Propagation Letters*, vol. 19, no. 10, pp. 1719–1723, 2020.

[17] F. N. Ayoub, Y. Tawk, E. Ardelean, J. Costantine, S. A. Lane, and C. G. Christodoulou, "Cross-slotted waveguide array with dual circularly polarized radiation at W-band," *IEEE Transactions on Antennas and Propagation*, vol. 70, no. 1, pp. 268–277, 2022.

[18] R. J. Mailloux, *Phased Array Antenna Handbook*, Artech House, Norwood, MA, USA, 2nd edition, 2005.

[19] H. Hu, X. Gao, and D. Fu, "A transformation technique from near-field to aperture-field based on FFT," *Journal of Microwaves*, vol. 17, no. 2, pp. 1–6, 2001.